Progress In Electromagnetics Research M, Vol. 45, 101–111, 2016

Scattering of Light by the Metal-Coated Dielectric Nanocylinders with Angular Periodicity

Vakhtang Jandieri[1, *], Kiyotoshi Yasumoto[2], Yunfei Liu[2], and Jaromir Pistora[1]

Abstract—Scattering of light by metal-coated dielectric nanocylinders periodically distributed along a cylindrical surface is investigated both theoretically and numerically. The structure is under the authors' interest because of its practical application in design and fabrication of plasmonic devices such as plasmonic ring resonators, Plasmonic Crystals and THz waveguides. The method is based on the T-matrix approach and the field expansion into the cylindrical Floquet modes. The method is rigorous, straightforward and can be easily applied to various cylindrical configurations with different types and locations of the excitation sources. Scattering cross section and absorption cross section of three and four silver (Ag) coated-dielectric nanocylinders periodically situated along a cylindrical surface are studied. Near field distributions are investigated at particular wavelengths corresponding to the resonance wavelengths in the spectral responses. Special attention is paid to the unique and interesting phenomena characterizing the cylindrical structure composed of the metal-coated nanocylinders such as: ***a***) localization of the field at the outer and inner interfaces of the metal-coated nanocylinders; ***b***) excitement of the field in the gap region between the nanocylinders through the coupled plasmon resonance and ***c***) strong confinement of the field inside the cylindrical structure. Detailed investigations have shown that unique phenomena characterizing the cylindrical configurations of the nanocylinders can be realized using a relatively simple structure composed of three nanocylinders and there is no need to further increase a number of the scatterers (nanocylinders).

1. INTRODUCTION

Interaction of light with the metallic nanostructures and nanoparticles gives rise to various unique effects in photonics and optoelectronics [1, 2]. Research of surface plasmons and their excitation is of interest in the studies of metamaterials, optical antennas and photonic crystals [3, 4]. The enhanced surface plasmon resonance in noble metallic systems at optical frequencies is expected to be a promising issue for realizing excellent scatterers and absorbers of the visible light [5–8]. Recently, much attention has been paid to the light scattering from metal-dielectric layered structures, because of their promising applications in sensors [9], super-scattering [10] and invisible cloaking [11, 12]. Surface plasmons are accompanied by localized enhancement of the electromagnetic field. They have ability to guide electromagnetic energy on length scales below the diffraction limit. This leads to developing metallic nanostructures that can control light at the nanoscale in direct analogy to traditional optical components such as lens, mirrors and waveguides. Many of these applications rely on a planar geometry in practice [13–19].

An alternative of the planar configuration is a cylindrical configuration. Recently, in the microwave region the authors have introduced a new type of bandgap structure — Cylindrical Electromagnetic Bandgap Structure [20] — composed of the perfect electric conductor (PEC) rods

Received 5 October 2015, Accepted 4 December 2015, Scheduled 21 December 2015
* Corresponding author: Vakhtang Jandieri (jandieri@ee.knu.ac.kr).
[1] Nanotechnology Centre, VSB-Technical University of Ostrava, 17. listopadu 15, 708 33 Ostrava-Poruba, Czech Republic. [2] College of Information Science and Technology, Nanjing Forestry University, Nanjing 210037, China.

periodically distributed along layered cylindrical surfaces. Formulation of boundary-value problem for the configuration composed of the PEC rods is quite different from that of the metallic rods in the optical region. In this regard, this manuscript is devoted to the investigation of the light scattering by metal-coated dielectric nanocylinders periodically distributed along the cylindrical surface. Authors believe that these studies could find practical application in the analyses of optical ring resonators [21, 22], cylindrical THz waveguides [23–25] and Plasmonic Crystals having cylindrical configuration. The rigorous formulation proposed in the manuscript uses T-matrix of a circular scatterer in isolation [26, 27] and it is taking into account all cylindrical Floquet modes and their interactions through the scattering between the nanocylinders periodically distributed along a circular ring [20, 28, 29]. It could be considered as the main advantage of the proposed formulation. Another advantage is that the method can be easily applied to various configurations of the layered cylindrical structures (Plasmonic Crystals) with different types and locations of the excitation sources. Our method is also applicable to the analyses of electromagnetic scattering by the multi-layer-coated nanocylinders. The extension is straightforward. We may replace the expression of the T-matrix of the coated nanocylinder by the T-matrix of the multi-layer-coated nanocylinder, which can be easily obtained using the recursive relation for the reflection and transmission coefficients of cylindrical waves at multilayered cylindrical surfaces. We have already conducted the preliminary studies about electromagnetic scattering on the multi-layer-coated nanocylinders.

An important point of worth mentioning is a comparison of the proposed formulation and the formulation used in the recent paper of our research group [30]. In [30] for two-cylinder systems the authors took into account the multiple interactions of the fields scattered from the individual cylinders by using the T-matrix and the translation matrices for cylindrical wave functions. The method is efficient when dealing with relatively small number of scatterers. However, if we directly apply this method to our structure, the calculation process becomes complicated and time-consuming especially when a number of the scatterers along the cylindrical surface is increasing. On the other hand, in our present manuscript the formulation is modified taking into account the *periodic nature* of the structure. In case of cylindrical structure with angular periodicity the problem is reduced to the calculation of a circulant matrix. Solving a linear system of equations it is enough to calculate a scattering amplitude for only one scatterer (nanocylinder). Scattering amplitudes for all other scatterers (nanocylinders) are easily obtained taking into account periodicity of the structure. Hence, a calculation process is greatly simplified.

Although our rigorous formulation is applicable to the analyses of light scattering by arbitrary number of the nanocylinders, we investigate up to four metal silver (Ag)-coated dielectric nanocylinders periodically located along the circular ring in a free space. Firstly, the scattering cross section (SCS) and the absorption cross section (ACS) of three and four metal-coated nanocylinders are studied at various distances between the nanocylinders keeping their radii the same. Note that the resonances appearing in the short wavelength region ($250\,\mathrm{nm} < \lambda < 400\,\mathrm{nm}$) correspond to the plasmon resonances of the metal-coated nanocylinders in isolation and the resonance wavelengths do not change by changing a separation distance between the nanocylinders. The spectral responses show number of interesting profiles characterizing the cylindrical configuration of the metal-coated nanocylinders. For instance, when a separation distance between the nanocylinders is small (nanocylinders are located very close, but not touching each other), there appear resonance peaks in the long wavelength region ($800\,\mathrm{nm} < \lambda < 2000\,\mathrm{nm}$) for both scattering and absorption cross sections. Shift of the resonances can be controlled by changing the separation distance between the nanocylinders located in a close vicinity. These resonances are characterized as the resonances intrinsic to the cylindrically periodic system. Other resonances appearing in the intermediate wavelength region ($400\,\mathrm{nm} < \lambda < 800\,\mathrm{nm}$) describe the resonant coupling of the surface plasmon fields in the multiple nanocylinders' systems.

Near field distributions are calculated at the particular wavelengths corresponding to the resonance wavelengths in spectral responses. A physical insight is given to: ***a***) enhancement of the near field at the inner (metal-dielectric) and outer (metal-free space) interfaces (corresponding to the resonances in the short wavelength region); ***b***) localization of the excited field in the gap region between the nanocylinders through the coupled plasmon resonance (corresponding to the resonances in the intermediate wavelength region); ***c***) strong confinement of the field inside the cylindrical structure (corresponding to the resonances in the long wavelength region). The latter uniquely characterizes the cylindrical configuration composed of the periodically distributed nanocylinders. All these above-mentioned properties are technologically important and could present significant contribution in the flexible design and fabrication of the optical plasmon devices.

Finally, it should be noted that recently Rahmani and co-workers have numerically and experimentally analyzed the electromagnetic scattering on various configurations of the cylindrical structure composed of Au nanoparticles [31]. The authors use the conventional numerical method (FDTD) to study the scattering and absorption characteristics, whereas our analysis is based on the rigorous formulation. Using the proposed formulation we can easily and in a very short time analyze various models of the multilayered cylindrical structures with arbitrary number of periodically distributed nanocylinders under different geometrical parameters. When the desired characteristics are observed, we will be able to implement the geometrical parameters under which the desired characteristics are obtained, in the numerical and experimental studies of the real world structures. It will substantially decrease time, effort and expenses needed for the detailed numerical and experimental investigations.

2. FORMULATION OF THE PROBLEM

A cross sectional view of N metal-coated dielectric nanocylinders periodically distributed on a circular ring having a radius R is shown in Fig. 1. The structure is located in a free space with material constants ε_0 and μ_0. Coaxial cylinder with outer radius r_1 consists of a circular dielectric core with radius r_2 and a metal coating layer of thickness $r_1 - r_2$. Material constants of the coating metal and dielectric core are denoted by (ε_M, μ_0) and (ε, μ_0), respectively and (ρ_j, ϕ_j) denote the local coordinate system for the j-th nanocylinder. The structure is illuminated by a plane wave of unit amplitude with an incident angle φ^i with respect to the x-axis. It is well known that the surface plasmons are excited in the case of $\mathbf{H}||z$. Solutions to the H_z field in the outer region $\rho_j > r_1$, inside the metal cover $r_2 < \rho_j < r_1$ and inside the dielectric core $\rho_j < r_2$ (Fig. 1) are obtained based on the superposition of the cylindrical waves.

Firstly, we write the solution to the H_z in the outer region of a free space $\rho_j > r_1$ in the following form:

$$H_z = \mathbf{\Phi}^T \cdot \mathbf{b} + \sum_{j=1}^{N} \mathbf{\Psi}_j^T \cdot \mathbf{G}_j \cdot \mathbf{b}, \quad \rho_j > r_1 \tag{1}$$

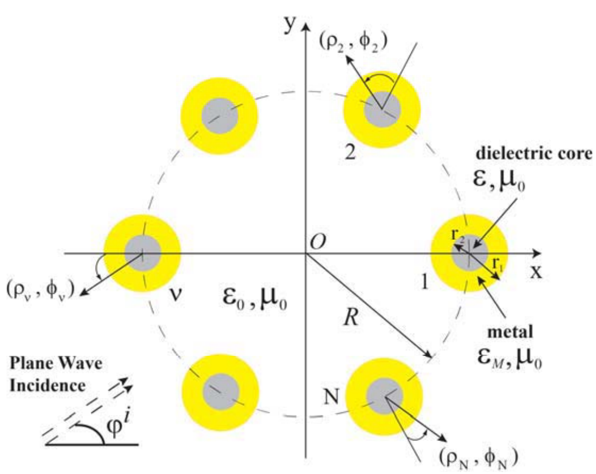

Figure 1. Cross-sectional view of N metal-coated dielectric nanocylinders periodically distributed on a circular ring with radius R. Material constants of the coating metal and dielectric core are denoted by $(\varepsilon_M, \mu_0, r_1)$ and $(\varepsilon, \mu_0, r_2)$, respectively and (ρ_j, ϕ_j) denote the local coordinates for the j-th nanocylinder. Excitation by a plane wave with incident angle φ^i is considered. A metal coating layer has a thickness $r_1 - r_2$.

with

$$\mathbf{\Phi} = \left[J_m(k_0\rho)e^{im\phi}\right], \quad \mathbf{\Psi}_j = \left[H_m^{(1)}(k_0\rho_j)e^{im\phi_j}\right] \tag{2}$$

$$\mathbf{b} = \left[i^m e^{-im\varphi^i}\right] \tag{3}$$

$$\mathbf{G}_j = \sum_{q=1}^{N} \boldsymbol{\sigma}_{q,j} \cdot \mathbf{T}^{(1)} \cdot \boldsymbol{\alpha}_q \tag{4}$$

$$\mathbf{T}^{(1)} = \mathbf{R}_{fm} + \mathbf{F}_{fm} \cdot \mathbf{R}_{md} \cdot (\mathbf{I} - \mathbf{R}_{mf} \cdot \mathbf{R}_{md})^{-1} \cdot \mathbf{F}_{mf} \tag{5}$$

$$\boldsymbol{\sigma}_{q,j} = \frac{1}{N} \sum_{\ell=1}^{N} \left(e^{-i(q-1)(\ell-1)\theta} (\mathbf{\Lambda}_\ell)^{-1}\right) e^{i(j-1)(\ell-1)\theta} \tag{6}$$

$$\boldsymbol{\alpha}_q = \left[(-1)^{m-n} J_{m-n}(k_0 R) e^{in(q-1)\theta}\right] \tag{7}$$

$$\mathbf{\Lambda}_\ell = \mathbf{I} + \sum_{p=2}^{N} e^{i(\ell-1)(p-1)\theta} \mathbf{A}_p \tag{8}$$

$$\mathbf{A}_p = -\mathbf{T}^{(1)} \cdot \boldsymbol{\kappa}_p \, (p = 2, 3, \ldots, N) \tag{9}$$

$$\boldsymbol{\kappa}_p = \left[(-1)^m H_{m-n}^{(1)}(k_0 d_p) e^{i(m+n)\zeta_p}\right] \tag{10}$$

$$\zeta_p = \pi/2 - (p-1)\theta/2 \tag{11}$$

$$d_p = 2R \sin[(p-1)\theta/2] \tag{12}$$

$$\rho = \sqrt{x^2 + y^2}, \quad \cos\phi = \frac{x}{\rho} \tag{13}$$

where k_0 is a wavenumber in a free space; $\mathbf{b}$ is an amplitude vector of the incident wave; (ρ, ϕ) denote the global cylindrical coordinate system; J_m and $H_m^{(1)}$ represent the Bessel and Hankel functions, respectively; $\mathbf{I}$ is an unit matrix; $\theta = 2\pi/N$ is an angle between the two nearest nanocylinders; $\mathbf{R}_{ij}$ and $\mathbf{F}_{ij}$ $(i, j = f, m, d)$ are diagonal matrices describing the reflection and transmission of the cylindrical waves from the region "j" into the region "i", where the indices "d", "m" and "f" denote dielectric, metal and free space, respectively. The explicit expressions for the diagonal reflection and transmission matrices are written in our recent work [30].

Solution to the H_z^j inside the metal cover $r_2 < \rho_j < r_1$ is written as follows:

$$H_z^j = \bar{\Phi}_j^T \cdot \mathbf{T}^{(2)} \cdot \left(\sum_{i=2}^{N} \boldsymbol{\kappa}_i \cdot \mathbf{G}_i + \alpha_1\right) \cdot \mathbf{D}_j \cdot \mathbf{b} + \bar{\Psi}_j^T \cdot \mathbf{T}^{(3)} \cdot \left(\sum_{i=2}^{N} \boldsymbol{\kappa}_i \cdot \mathbf{G}_i + \boldsymbol{\alpha}_1\right) \cdot \mathbf{D}_j \cdot \mathbf{b}, \quad r_2 < \rho_j < r_1 \tag{14}$$

with

$$\bar{\Phi}_j = \left[J_m(k_M\rho_j)e^{im\phi_j}\right], \quad \bar{\Psi}_j = \left[H_m^{(1)}(k_M\rho_j)e^{im\phi_j}\right] \tag{15}$$

$$\mathbf{D}_j = \left[e^{in(j-1)\theta}\delta_{nn'}\right] \tag{16}$$

$$\mathbf{T}^{(2)} = (\mathbf{I} - \mathbf{R}_{mf} \cdot \mathbf{R}_{md})^{-1} \cdot \mathbf{F}_{mf} \tag{17}$$

$$\mathbf{T}^{(3)} = \mathbf{R}_{md} \cdot (\mathbf{I} - \mathbf{R}_{mf} \cdot \mathbf{R}_{md})^{-1} \cdot \mathbf{F}_{mf} \tag{18}$$

where $k_M = k_0\sqrt{\varepsilon_M}$ and $\delta_{nn'}$ is the Kronecker's delta.

Finally, solution to the H_z^j inside the dielectric core $\rho_j < r_2$ is expressed in the following form:

$$H_z^j = \tilde{\Phi}_j^T \cdot \mathbf{T}^{(4)} \cdot \left(\sum_{i=2}^{N} \boldsymbol{\kappa}_i \cdot \mathbf{G}_i + \boldsymbol{\alpha}_1\right) \cdot \mathbf{D}_j \cdot \mathbf{b}, \quad \rho_j < r_2 \tag{19}$$

with

$$\tilde{\Phi}_j = \left[J_m(k\rho_j) e^{im\phi_j} \right] \tag{20}$$

$$\mathbf{T}^{(4)} = \mathbf{F}_{dm} \cdot (\mathbf{I} - \mathbf{R}_{mf} \cdot \mathbf{R}_{md})^{-1} \cdot \mathbf{F}_{mf} \tag{21}$$

where $k = k_0\sqrt{\varepsilon}$.

3. NUMERICAL RESULTS AND DISCUSSIONS

In the numerical examples we assume silver (Ag) for the metal employing the Drude-Lorentz model [19, 32]. Silver is commonly used for nanoparticle plasmonics because of the relatively easy production and small loss. An incidence of the plane waves at $\varphi^i = 0^0$ (from negative x-axis) is studied under the following structural parameters: $r_1 = 60$ nm, $r_2 = 45$ nm and $\varepsilon = 2.25\varepsilon_0$ (glass core). Although the developed formulation can be applied to an arbitrary number of nanocylinders periodically situated along a cylindrical surface, the light scattering on three and four metal (Ag)-coated nanocylinders is investigated in the manuscript. Firstly, SCS and ACS [28–30] of three metal (Ag)-coated nanocylinders are plotted in Fig. 2 in the wavelength range from 250 nm to 2000 nm at four different values of radius R: $R = 100$ nm (nanocylinders are well separated), $R = 72$ nm and $R = 70$ nm (nanocylinders are located in a close vicinity, but not touching each other) and $R = 69.2820$ nm (nanocylinders are touching). From Fig. 2 it follows that SCS and ACS have the resonance peaks at the wavelengths $\lambda = 300$ nm and $\lambda = 330$ nm for all values of radius R. Resonances in the short wavelength region characterize the plasmon resonances of the metal (Ag)-coated nanocylinders in isolation [19 (Fig. 2)] and therefore, the resonance wavelengths do not change by changing a separation distance between the nanocylinders. It should be noted that when the nanocylinders are well separated $R = 100$ nm, SCS has one pronounced resonance peak at $\lambda = 650$ nm (black line). However, when the separation distance between the nanocylinders decreases, it splits into two peaks at $\lambda = 575$ nm, $\lambda = 705$ nm when $R = 72$ nm (blue line), at $\lambda = 590$ nm, $\lambda = 740$ nm when $R = 70$ nm (red line) and at $\lambda = 630$ nm, $\lambda = 780$ nm when $R = 69.2820$ nm (gray line). Note that the first peaks are formed due to the coaxial nature of the metal-coated nanocylinders [19 (Fig. 2)], whereas the second resonance peaks in the intermediate wavelength region are due to the resonant coupling of the surface plasmon fields in the multiple nanocylinders' systems. It is important to mention that when the nanocylinders are located quite close but not touching each other at $R = 72$ nm (blue line) and $R = 70$ nm (red line), SCS and ACS have the resonances in the long wavelength region at $\lambda = 950$ nm and $\lambda = 1300$ nm, respectively. These resonances are characterized as the resonances intrinsic to the cylindrically periodic system. Note that there are no resonance peaks in the long wavelength region when the nanocylinders are well separated.

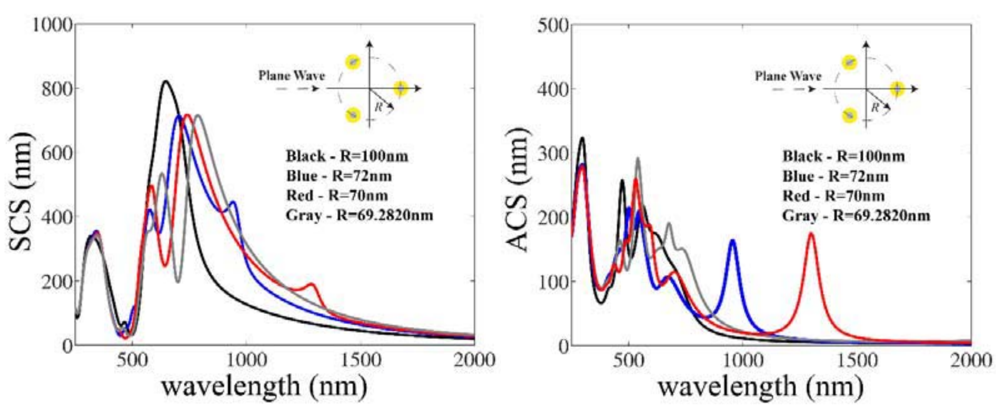

Figure 2. Scattering cross section (SCS) and absorption cross section (ACS) of three metal (Ag)-coated dielectric nanocylinders as functions of the wavelength at $r_1 = 60$ nm, $r_2 = 45$ nm, $\varepsilon = 2.25\varepsilon_0$ and $\varphi^i = 0^0$ for different values of R: $R = 100$ nm (black line), $R = 72$ nm (blue line), $R = 70$ nm (red line) and $R = 69.2820$ nm (gray line).

In order to give a physical insight into the analyses of the spectral responses, we study the near field distributions $|H_z|$ at particular resonance wavelengths shown in Fig. 2. The circles depicted by white lines indicate the boundary surfaces of the metal (Ag)-coated coaxial nanocylinders. From Fig. 3(a) and Fig. 3(b) it follows that when the nanocylinders are well separated $R = 100$ nm the surface plasmon supported by the interface between the metal and the free space resonates to the incident plane wave. A strong field is excited in the illuminated side of the nanocylinders at the resonances in the short wavelength region at $\lambda = 300$ nm (resonance wavelength in ACS) and at $\lambda = 330$ nm (resonance wavelength in SCS). At the resonances in the intermediate wavelength region an effect of the coaxial nature of the nanocylinders becomes significant. Incident waves penetrate through the metal layer and the excited field is localized along the interface between the dielectric core and the coating metal (Ag) layer at $\lambda = 472$ nm (resonance peak in the ACS) and at $\lambda = 650$ nm (resonance peak in the SCS) as shown in Fig. 3(c) and Fig. 3(d), respectively. It should be noted that there is no interference between the near fields scattered from the individual nanocylinders at $\lambda = 472$ nm and the field is strongly localized only at the interfaces between the dielectric core and the coating metal (Ag) layer. On the

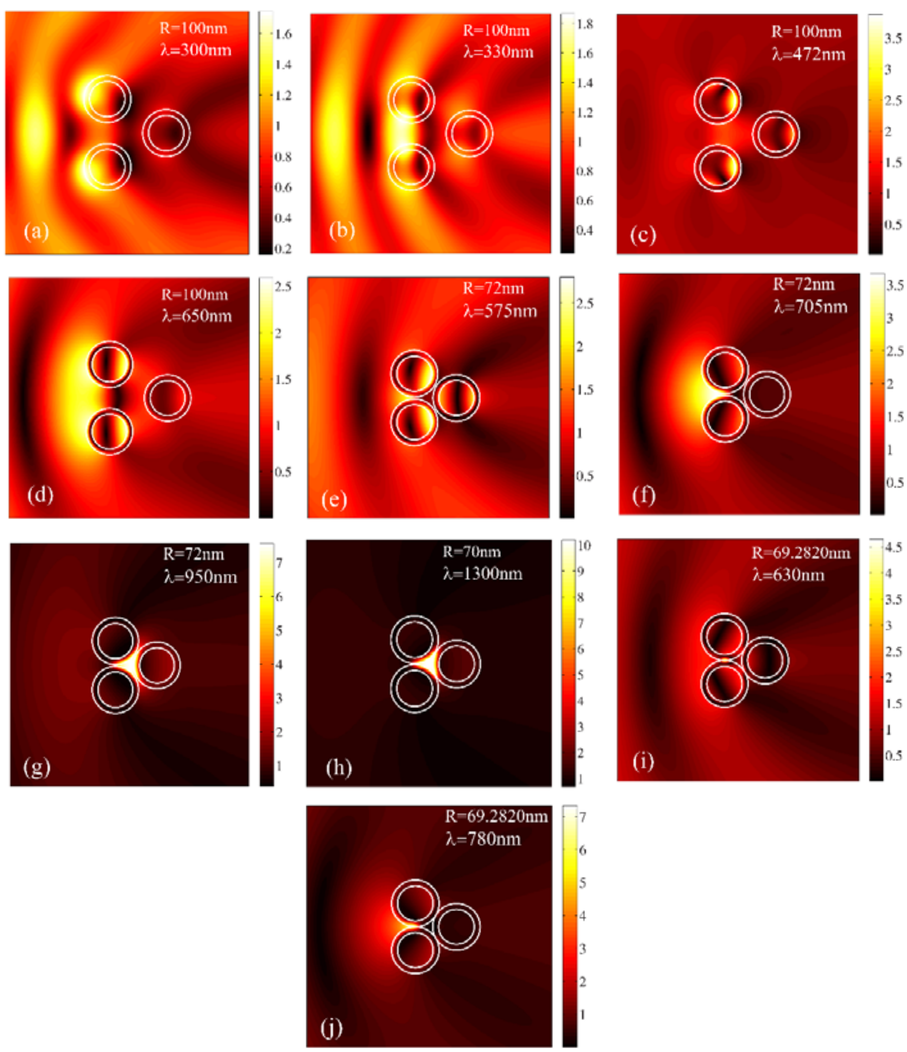

Figure 3. Near field distributions $|H_z|$ of three metal (Ag)-coated nanocylinders periodically situated along the cylindrical surface at the resonance wavelengths of the spectral response (Fig. 2) for different values of radius R: $R = 100$ nm (Fig. 3(a)–Fig. 3(d)), $R = 72$ nm (Fig. 3(e)–Fig. 3(g)), $R = 70$ nm (Fig. 3(h)) and $R = 69.2820$ nm (Fig. 3(i), Fig. 3(j)). The plane waves are incident on the structure from the negative x-axis.

other hand, there is a resonant coupling of the surface plasmon fields in the nanocylinders' systems at $\lambda = 650\,\text{nm}$.

Figures 3(e)–3(g) show the near field distributions $|H_z|$ when the nanocylinders are located very close but not touching each other $R = 72\,\text{nm}$. Near field distribution at the resonance wavelength $\lambda = 575\,\text{nm}$ (resonance wavelength in SCS) is shown in Fig. 3(e). The field is strongly localized at the surface between the metal cover and the dielectric core of the nanocylinders located at the illuminating side of the incident plane waves. Multiple interactions between the nanocylinders are hardly observed. However, the incident plane wave resonates to the coupled surface plasmon modes supported in the gap between two nanocylinders at $\lambda = 705\,\text{nm}$ and the localized field is strongly enhanced in a small region between the nanocylinders (Fig. 3(f)). Illumination at the right-side is blocked by two nanocylinders and therefore, the major contribution in the field formation is governed only by these two metal scatterers. It is important to note that the field inside the region surrounded by three nanocylinders is almost zero.

A very interesting effect is observed at $\lambda = 950\,\text{nm}$ (resonance wavelength in SCS and ACS), when the localized field is strongly enhanced inside the region around the global origin surrounded by the three metal-coated nanocylinders. This effect is demonstrated in Fig. 3(g). In order to study a strong field confinement inside the cylindrical periodic structure in a more detail, we further slightly decrease a distance between the nanocylinders. Near field distribution at the resonance wavelength $\lambda = 1300\,\text{nm}$ when $R = 70\,\text{nm}$ is illustrated in Fig. 3(h). It could be vividly seen that the field localization inside the cylindrical structure is much stronger than that in Fig. 3(g). It is very important to note that in order to realize a strong field confinement inside the cylindrical structure we should have a very small gap between the nanocylinders because the surface plasmon field extends over the metal region and the free space. Effect of the strong field confinement could be considered as a unique feature for the cylindrical configuration composed of the nanocylinders. When the nanocylinders are touching each other at $R = 69.2820\,\text{nm}$ there is no small gap between them and the field cannot penetrate inside the structure. The surface plasmons on the outer metal interfaces are strongly coupled and a new surface plasmon mode is formed in the touching region. This effect is demonstrated in Figs. 3(i) and 3(j). All these above-mentioned features could be considered as technologically important to flexibly design and fabricate the plasmonic waveguides and plasmonic resonators.

In order to discuss the light interaction through the plasmon resonant coupling in metal (Ag)-coated dielectric nanocylinders in more detail, we analyze the scattering characteristics by four nanocylinders periodically distributed along the circular ring. The SCS and ACS are plotted in Fig. 4 at four different values of radius R: $R = 120\,\text{nm}$ (nanocylinders are well separated), $R = 95\,\text{nm}$ and $R = 85.5\,\text{nm}$ (nanocylinders are located in a close vicinity, but not touching each other) and $R = 84.8528\,\text{nm}$ (nanocylinders are touching). From Fig. 4 it follows that the spectral responses demonstrate similar properties as those for the three nanocylinders illustrated in Fig. 2. The near field distributions $|H_z|$ of

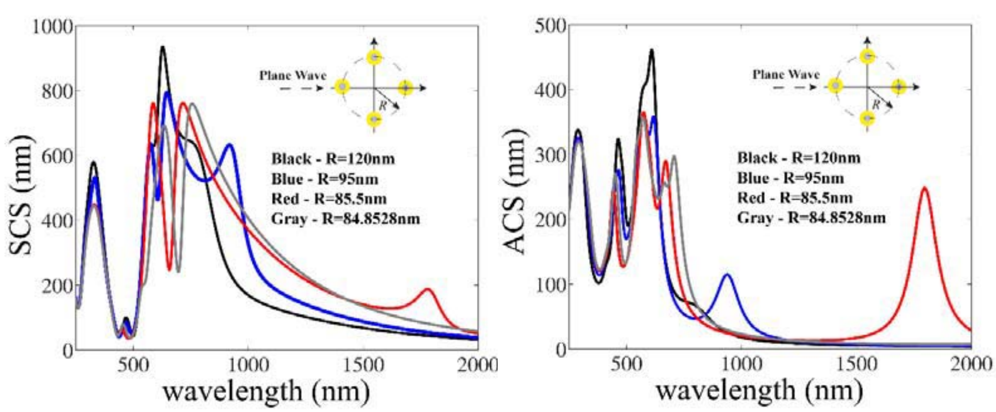

Figure 4. Scattering cross section (SCS) and absorption cross section (ACS) of four metal (Ag)-coated nanocylinders as functions of the wavelength for different values of R: $R = 120\,\text{nm}$ (black line), $R = 95\,\text{nm}$ (blue line), $R = 85.5\,\text{nm}$ (red line) and $R = 84.8528\,\text{nm}$ (blue line). Other parameters are the same as those in Fig. 2.

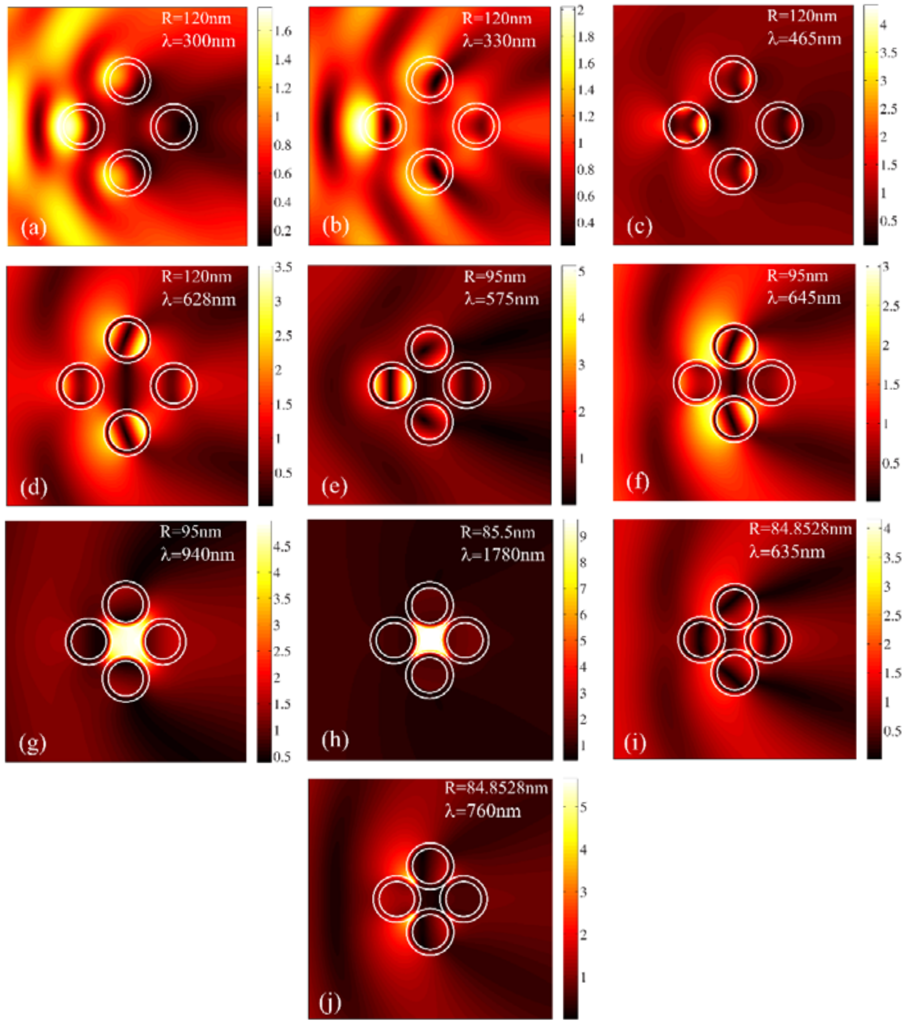

Figure 5. Near field distributions $|H_z|$ of four metal (Ag)-coated nanocylinders periodically situated along the cylindrical surface at the resonance wavelengths of the spectral response (Fig. 4) for different values of radius R: $R = 120\,\text{nm}$ (Fig. 5(a)–Fig. 5(c)), $R = 95\,\text{nm}$ (Fig. 5(d)–Fig. 5(g)), $R = 85.5\,\text{nm}$ (Fig. 5(h)) and $R = 84.8528\,\text{nm}$ (Fig. 5(i), Fig. 5(j)). The plane waves are incident on the structure from the negative x-axis.

four metal (Ag)-coated nanocylinders at the particular resonance wavelengths of the spectral responses (Fig. 4) are shown in Fig. 5. The figures vividly demonstrate that unique phenomena characterizing the cylindrical structures of metal-coated nanocylinders such as: ***a***) excitement of the field in the gap region through the coupled plasmon resonances; ***b***) localization of the field at the inner and outer interfaces of the metal; ***c***) strong confinement of the field inside the structure could be realized by properly adjusting the distance between the metal-coated nanocylinders keeping other geometrical parameters the same.

Electric field amplitude distributions for (a) three and four (b) metal-coated nanocylinders are plotted in Fig. 6. Other geometrical parameters are the same as those in Fig. 3(h) and Fig. 5(h) for the magnetic field. Finally, it is important to note that the similar analyses have been conducted for up to 12 metal-coated nanocylinders periodically distributed along the cylindrical surface. Our studies have shown that no new additional unique features are observed by increasing a number of the nanocylinders. From our investigations we may conclude that unique phenomena characterizing the cylindrical structures can be realized using a relatively simple configuration composed of three nanocylinders and there is no need to further increase a number of the nanocylinders.

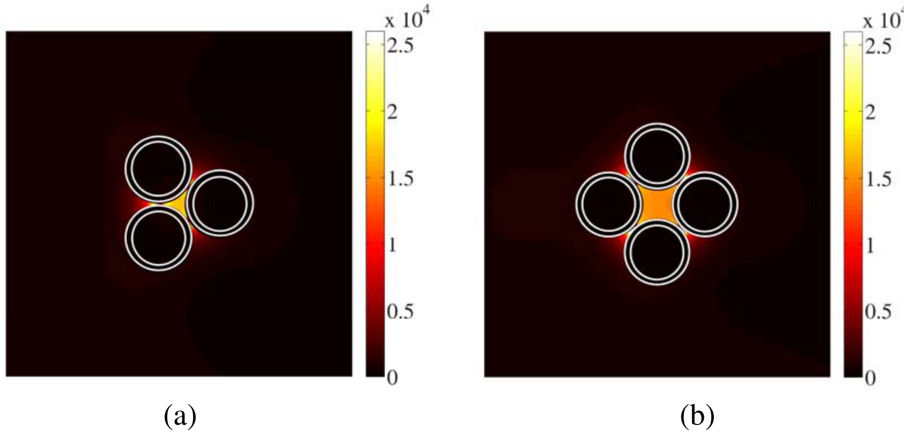

Figure 6. Electric field amplitude distribution $\sqrt{|E_\rho|^2 + |E_\phi|^2}$ of (a) three and (b) four metal (Ag)-coated nanocylinders periodically situated along the cylindrical surface. Other parameters are the same as those in Fig. 3(h) and Fig. 5(h).

4. CONCLUSION

A rigorous and accurate formulation for the light scattering by the plasmonic nanocylinders with angular periodicity has been presented. Cylindrical structures formed by the metal (silver)-coated dielectric nanocylinders periodically distributed along the cylindrical surface have been investigated from the viewpoint of flexible design and fabrication of optical devices such as THz waveguides, plasmonic ring resonators and Plasmonic Crystals. Scattering and absorption cross sections, as well as the near field distributions at the particular wavelengths associated with the resonance wavelengths in the spectral responses have been studied. The proposed formulation is straightforward, which could be considered as the main advantage of our formulation. The method could be easily generalized to the analyses of electromagnetic scattering, guidance and radiation by Plasmonic Crystals of cylindrical configuration (multilayered cylindrical structure composed of the nanocylinders) with arbitrary excitation sources and location of the sources with respect to the structure. Although the fabrication of the effective plasmonic devices is still quite difficult because of a high loss, Plasmonic Crystals as well as THz waveguides are under the extensive research interest. Authors believe that development of the formulation that is rigorous and not time-consuming could contribute in better understanding of electromagnetic scattering phenomena in the plasmonic structures having cylindrical symmetry.

ACKNOWLEDGMENT

This work was supported by grant of Moravia-Silesia region (MK9334523), the Grant Agency of the Czech Republic (P205/11/2137), and IT4 Innovations Centre of Excellence project (CZ.1.05/1.1.00/02.0070).

REFERENCES

1. Zhang, J. and L. Zhang, "Nanostructures for surface plasmons," *Advances in Optics and Photonics*, Vol. 4, 157, 2012.
2. Berini, P., "Long-range surface plasmon polaritons," *Advances in Optics and Photonics*, Vol. 1, 484, 2009.
3. Hess, O., J. Pendry, S. Maier, R. Oulton, J. Hamm, and K. Tsakmakidis, "Active nanoplasmonic materials," *Nature Materials*, Vol. 11, 573, 2012.
4. Berini, P. and I. De Leon, "Surface plasmon-polariton amplifiers and lasers," *Nature Photonics*, Vol. 6, 16, 2012.

5. Kravets, V., F. Schedin, and A. Grigorenko, "Extremely narrow plasmon resonances based on diffraction coupling of localized plasmons in arrays of metallic nanoparticles," *Physical Review Letters*, Vol. 101, 087403, 2008.
6. Luk'yanchuk, B. and V. Ternovsky, "Light scattering by a thin wire with a surface-plasmon resonance: Bifurcations of the Poynting vector field," *Physical Review B*, Vol. 73, 235432, 2006.
7. Nguyen-Huu, N., M. Cada, and J. Pistora, "Imperfectly geometric shapes of nanograting structures as solar absorbers with superior performance for solar cells," *Optics Express*, Vol. 22, A282, 2014.
8. Brongersma, M., Y. Cui, and S. Fan, "Light management for photovoltaics using high-index nanostructures," *Nature Materials*, Vol. 13, 451–460, 2014.
9. Velichko, E. and A. Nosich, "Refractive-index sensitivities of hybrid surface-plasmon resonances for a core-shell circular silver nanotube sensor," *Optics Letters*, Vol. 38, 4978, 2013.
10. Ruan, Z. and S. Fan, "Superscattering of light from subwavelength nanostructures," *Physical Review Letters*, Vol. 105, 013901, 2010.
11. Mirzaei, A., I. V. Shadrivov, A. E. Miroshnichenko, and Y. S. Kivshar, "Cloaking and enhanced scattering of core-shell plasmonic nanowires," *Opt. Express*, Vol. 21, 10454, 2013.
12. Okada, N. and J. Cole, "Cylindrical invisibility cloak based on photonic crystal layers that permits communication with the outside," *J. Opt. Soc. Am. B*, Vol. 29, 3344, 2012.
13. Nguyen-Huu, N., M. Cada, J. Pistora, and K. Yasumoto, "Tunable optical filter based on gold and silver double-sided gratings and its application as plasmonic sensor," *Journal of Lightwave Technology*, Vol. 32, 3477, 2014.
14. Zhang, J., J. Ou, K. MacDonald, and N. Zheludev, "Optical response of plasmonic relief meta-surfaces," *Journal of Optics*, Vol. 14, 114002, 2012.
15. Natarov, D., R. Sauleau, and A Nosich, "Periodicity-enhanced plasmon resonances in the scattering of light by sparse finite gratings of circular silver nanowires," *IEEE Photonics Technology Letters*, Vol. 24, 43, 2012.
16. Liu, H., X. Sun, Y. Pei, F. Yao, and Y. Jiang, "Tunability and linewidth sharpening of plasmon resonances on a periodic gold nanowire array coupled to a thin textured silver film," *Applied Physics B*, Vol. 104, 665, 2011.
17. D'Aguanno, G. and N. Mattiucci, "Dispersive and scattering properties of multilayer arrays made of plasmonic nanoparticles," *J. Opt. Soc. Am. B*, Vol. 31, 2524, 2014.
18. Natarov, D., V. Byelobrov, R. Sauleau, T. Benson, and A. Nosich, "Periodicity-induced effects in the scattering and absorption of light by infinite and finite grating of circular silver nanowires," *Optics Express*, Vol. 19, 22, 22176, 2011.
19. Jandieri, V., P. Meng, K. Yasumoto, and Y. Liu, "Scattering of light by gratings of metal-coated circular nanocylinders on a dielectric substrate," *Journal of the Optical Society of America A*, Vol. 32, 1384, 2015.
20. Jandieri, V., K. Yasumoto, and Y. Liu, "Directivity of radiation of a dipole source coupled to cylindrical electromagnetic bandgap structures," *J. Opt. Soc. Am. B*, Vol. 29, 2622, 2012.
21. Bozhevolnyi, S., V. Volkov, E. Devaux, J. Laluet, and T. Ebbesen, "Channel plasmon subwavelength waveguide components including interferometers and ring resonators," *Nature Letters*s, Vol. 440, 508, 2006.
22. Talebi, N., A. Mahjoubfar, and M. Shahabadi, "Plasmonic ring resonator," *J. Opt. Soc. Am. B*, Vol. 25, No. 12, 2116, 2008.
23. Atakaramians, S., S. Afshar V., T. M. Monro, and D. Abbott, "Terahertz dielectric waveguides," *Advances in Optics and Photonics*, Vol. 5, 169, 2013.
24. Mitrofanov, O., R. James, F. Anibal Fernandez, T. K. Mavrogordatos, and J. Harrington, "Reducing transmission losses in hollow THz waveguides," *IEEE Transactions on Terahertz Science and Technology*, Vol. 1, No. 1, 124, 2011.
25. Mitrofanov, O. and J. Harrington, "Dielectric-lined cylindrical metallic THz waveguides: Mode structure and dispersion," *Optics Express*, Vol. 18, No. 3, 1898, 2010.

26. Yasumoto, K., H. Toyama, and T. Kushta, "Accurate analysis of two-dimensional electromagnetic scattering from multilayered periodic arrays of circular cylinders using lattice sums technique," *IEEE Transactions on Antennas and Propagation*, Vol. 52, 2603, 2004.
27. Yasumoto, K., ed., *Electromagnetic Theory and Applications for Photonic Crystals*, CRC Press, Boca Raton, FL, 2005.
28. Jandieri, V. and K. Yasumoto, "Analysis of scattering from a finite array of circular cylinders using a model of layered cylindrical arrays," *Optics Communications*, Vol. 284, 4109, 2011.
29. Jandieri, V. and K. Yasumoto, "Electromagnetic scattering by layered cylindrical arrays of circular rods," *IEEE Transactions on Antennas and Propagation*, Vol. 59, 2437, 2011.
30. Meng, P., K. Yasumoto, and Y. Liu, "Surface plasmon resonant scattering in metal-coated dielectric nanocylinders," *Optics Communications*, Vol. 332, 18, 2014.
31. Rahmani, M., D. Lei, V. Giannini, B. Lukiyanchuk, M. Ranjbar, T. Liew, M. Hong, and S. Maier, "Subgroup decomposition of plasmonic resonances in hybrid oligomers: Modeling the resonance lineshape," *Nano Letters*, Vol. 12, 2101, 2012.
32. Laroche, T. and C. Girard, "Near-field optical properties of single plasmonic nanowires," *Appl. Phys. Lett.*, Vol. 89, 233119, 2006.